Urban Ecosystems (2021) 24:767–778
https://doi.org/10.1007/s11252-020-01073-4

Microclimate in an urban park and its influencing factors: a case study of Tiantan Park in Beijing, China

Yilun Li [1,2] · Shuxin Fan [1,2] · Kun Li [1,2] · Yue Zhang [1,2] · Li Dong [1,2]

Accepted: 17 November 2020 / Published online: 26 November 2020

Abstract

Construction of urban green spaces may effectively mitigate urban heat island effect. Better design of green spaces may improve their thermal performance, and therefore provide better ecosystem services in cities. Aiming at providing empirical evidence and further insights for urban park design, field measurement of air temperature (Ta) and relative humidity (Rh) was conducted in Tiantan Park in Beijing, China. Results show that within Tiantan park, 1.29–2.71 °C air temperature difference and 1.27–5.16% relative humidity difference were observed at different time. Among all parameters, radiation condition ($\beta = 0.872$; $\beta = 0.723$) and land cover composition ($\beta = 0.601$) are dominant influencing factor on daytime and nighttime Ta respectively. Among different vegetation types, deciduous trees have significant cooling and humidifying effects at noon in summer ($\rho = -0.65$); evergreen trees have little effects in summer, but a humidifying effect in winter ($\rho = -0.58$); grassland may give rise to daytime Ta in both summer and winter ($\rho = 0.48$; $\rho = 0.52$). Effects of the shape of different vegetation types remain unclear, while more compact imperious surfaces may lead to lower daytime Ta ($\rho = 0.55$; $\rho = 0.67$). Understanding such microclimate conditions in an urban park may assist designers to create a more thermally friendly environment in future.

Keywords Urban green space · Thermal environment · Air temperature · Relative humidity · The Temple of heaven

Introduction

Human activities have induced global climate change. By 2017, compared with pre-industrial period, the world has experienced a 0.8–1.2 °C temperature increase (Allen et al. 2018). Global warming leads to loss of biodiversity, extreme meteorological events etc., which are all potential threats to human beings (Costello et al. 2009; Patz et al. 2005). Cities with dense population and strong human activities are facing even more challenges. Although cities account for only 2% of global area, more than 50% of world population reside in cities (UN 2019), and it is estimated that 20–40% world population have experienced a temperature increase greater than 1.5 °C (Allen et al. 2018). A large number of man-made constructions have changed the thermal properties of underlying surfaces, caused poor ventilation and released a large number of anthropogenic heats, resulting in significantly higher air temperature (Ta) in cities than in rural areas, which is commonly known as urban heat island (UHI) effect (Oke et al. 1989).

Urban greening has long been proved as an effective way to regulate thermal environment and enhance thermal comfort as well as human perception (Bartesaghi Koc et al. 2018; Bowler et al. 2010; Gago et al. 2013; Hami et al. 2019). Studies have implemented various methods to investigate factors on urban greening's cooling and humidifying effects. Remotely sensed data were wildly used to investigate thermal performance of different landscape pattern on city scale (Masoudi and Tan 2019; Sun and Chen 2017; Xu et al. 2017). While field measurements and simulation are usually used at local and micro scale to investigate influence of land cover composition (Huang et al. 2008; Toparlar et al. 2018; Yan et al. 2014b), radiation condition (Cohen et al. 2012; Kong et al. 2016; Morakinyo et al. 2017), albedo (Taha 1997), urban geometry (Jamei et al. 2016; Johansson 2006; Taleghani et al. 2014), etc. on urban climate. Results of such studies may provide insight for urban planning and design.

Urban parks, an assemblage of abundant vegetation, have pronounced effects on local and micro scale climate. Previous empirical studies have proved that parks not only are cold and

✉ Li Dong
dongli@bjfu.edu.cn

[1] School of Landscape Architecture, Beijing Forestry University, Beijing 10083, China

[2] Beijing Laboratory of Urban and Rural Ecological Environment, Beijing, China

wet islands in cities, but can influence its vicinity areas (Barradas 1991; Chang et al. 2007; Jansson et al. 2007; Potchter et al. 2006; Yan et al. 2018). Most of the studies on urban park's thermal performance implement simulation method and have investigated how different configurations of landscape elements (i.e. vegetation, pavement, etc.) and vegetation types (deciduous and evergreen trees, shrubs and turf) may influence park's thermal performance (Sodoudi et al. 2018; Sun et al. 2017; Toparlar et al. 2018; Afshar et al. 2018). Nevertheless, only a few empirical researches have been conducted to investigate thermal environment within urban parks (Barradas 1991; Bilgili et al. 2013; Hwang et al. 2015). Barradas (1991) depicted Ta distribution within five parks in Mexico City with isotherms, and found correlation between Ta difference and park size. Bilgili et al. (2013) depicted the Ta distribution in three parks in Turkey, and found that Ta was correlated with vegetation cover. Hwang et al. (2015) measured Ta in 10 urban parks in Singapore and found that shading is the important factor in reducing temperatures by comparing the characteristics of hot and cold spots. Further empirical studies are still in need when considering that a majority of prevalent simulation studies lack validation (Toparlar et al. 2017), and many questions remain to be answered. It is yet unclear whether there is stable temperature or humidity gradient in urban parks. And the dominant factor on thermal environment in urban parks has not been identified. In different climate zones, the above results may also be inconsistent and in need of further research.

Beijing is a megacity with a temperate climate that has undergone rapid urbanization in the last few decades. The total population has reached 21.71 million in 2017, and the proportion of urban population has increased from 73.44% in 1990 to 86.45% in 2017 (NBSC 2018). Such vast urbanization has exacerbated UHI effect in Beijing (Liu et al. 2007; Peng et al. 2016). Urban parks may provide more thermally comfortable places for city dwellers especially in hot summers (Hami et al. 2019). Better configuration of landscape elements may enhance urban parks' ecological and recreational functions. And better design and management of urban parks may reinforce its ability to confront extreme weather conditions.

Therefore, in order to provide empirical evidence of the influencing factor on microclimate in an urban park which can be compared with previous simulation studies, and further provide insight for designers and park managers, and thus create a more comfortable environment for citizens, we conducted field measurements within an urban park in Beijing during daytime and nighttime in both summer and winter. Specifically, we hope to find answers to the following questions: (1) How are Ta and relative humidity (Rh) distributed within an urban park? (2) How do spatial location, radiation condition and land cover composition affect microclimate in an urban park? (3) What is the dominant influencing factor on Ta and Rh at different time? (4) How different types of vegetation may contribute to microclimate in an urban park?

Methodology

Site location

Beijing (39°56'N, 116°20'E) is located in the northwest of North China Plain, with a total area of 16,410 km^2. It features a warm temperate semi humid continental monsoon influenced climate, with long summers and winters and relatively short springs and autumns. In 2017, the precipitation was 576.2 mm and the annual average air temperature was 14.2 °C (NBSC 2018).

Taking park size, location and composition into consideration, Tiantan Park was selected as the study site. Tiantan Park, also known as The Temple of Heaven, with a total area of 198 ha, is located within the 2nd Ring Road and near the center of Beijing, surrounded by densely built urban environment. Vegetation in Tiantan Park is exuberant, as its history may date back to approximately 600 years ago. There are more than 1100 trees that are over 300 years old (MOTTH 2002). Tiantan Park also features abundant evergreen trees, which are mainly *Juniperus chinensis*, *Platycladus orientalis* and *Pinus tabuliformis*. As one of the 11 municipal parks in Beijing, Tiantan Park serves as an important recreational place for citizens and surrounding residents.

Another reason that this specific park was chosen is that it is composed simply of vegetation and impervious surfaces but no water bodies. Water bodies have strong ability to absorb radiation energy (Oke 1992). Previous empirical studies have proved that water bodies have strong impacts on local and micro scale climate (Hathway and Sharples 2012; Saaroni and Ziv 2003). Therefore, to avoid the impact of large water bodies and to fully investigate vegetation's thermal effect, we intentionally selected Tiantan Park as the study site.

Measurement of air temperature and relative humidity

Ta and Rh were measured with Fluke 971 Temperature Humidity Meter. The accuracy of the device is ±0.5 °C and ± 2.5%, and the resolution is 0.1 °C and 0.1%, meeting the requirements of ISO 7726 (ISO 1998). The sensor of the device is surrounded by a porous black shield which may both provide protection and partly avoid direct exposure to sunshine. And to further avoid the influence of direct exposure to sunshine, we took a sunshade which is covered with black coating during data collection. Ta and Rh were collected at the height of 1.2 m.

Measurements were taken on three clear and windless days that had similar weather conditions in summer (July, 2019) and winter (February, 2019). Survey times were at noon starting at 13:00, and at night starting at 21:00 in summer and 20:00 in winter. We intentionally chose a route on the main path that traveled through both the innermost and outermost of the park, and to avoid dramatic weather condition change during sampling, each sampling process was restricted to approximately 60 min. Due to the park administration policy that the core Temple area closes at dusk, making it hard to travel from the west part to the east, the majority of points were selected on the west. Measurement started from an open square near the south entrance (S01) and each two adjacent sampling points were approximately 100-150 m apart. At each point, Ta and Rh were recorded only after the device had stabilized. Figure 1 shows the location of all sampling points.

Considering that the measurements at each point were not simultaneous, at the start and end of each measurement process, three Ta and Rh were measured at S01 with 30s interval to represent the starting and ending time Ta and Rh. Ta and Rh were presumed to have changed linearly during data sampling, and the rate of Ta and Rh change was used to adjust all measurements to the starting time of each measurement process.

Measurement of influencing factors

Numerous factors influence thermal environment. In this research, we mainly focused on three types of influencing factors, which are spatial location of sampling points, radiation condition above sampling points and land cover features around sampling points. Worldview-3 image with four multi-spectral bands (1.24 m resolution) and 1 panchromatic band (0.31 m resolution) acquired on February 21, 2019 and GF-2 image with four multi-spectral bands (4 m resolution) and 1 panchromatic band (0.8 m resolution) acquired on September 5, 2018 were used for visual interpretation.

Spatial location is represented by the distance from sampling points to park boundary (DTB) and the distance from sampling points to park geometric center (DTC). Park's boundary was visually interpreted and the geometric center and all distances were calculated by using Arc GIS 10.2.

Radiation condition is represented by sky view factor (SVF) and sunshine duration (SD). Fisheye photographs were taken with Canon EOS 5D and Sigma 8 mm F3.5 fisheye lens at each sampling point at the height of 1.2 m in July and February respectively. SVF and SD was calculated by

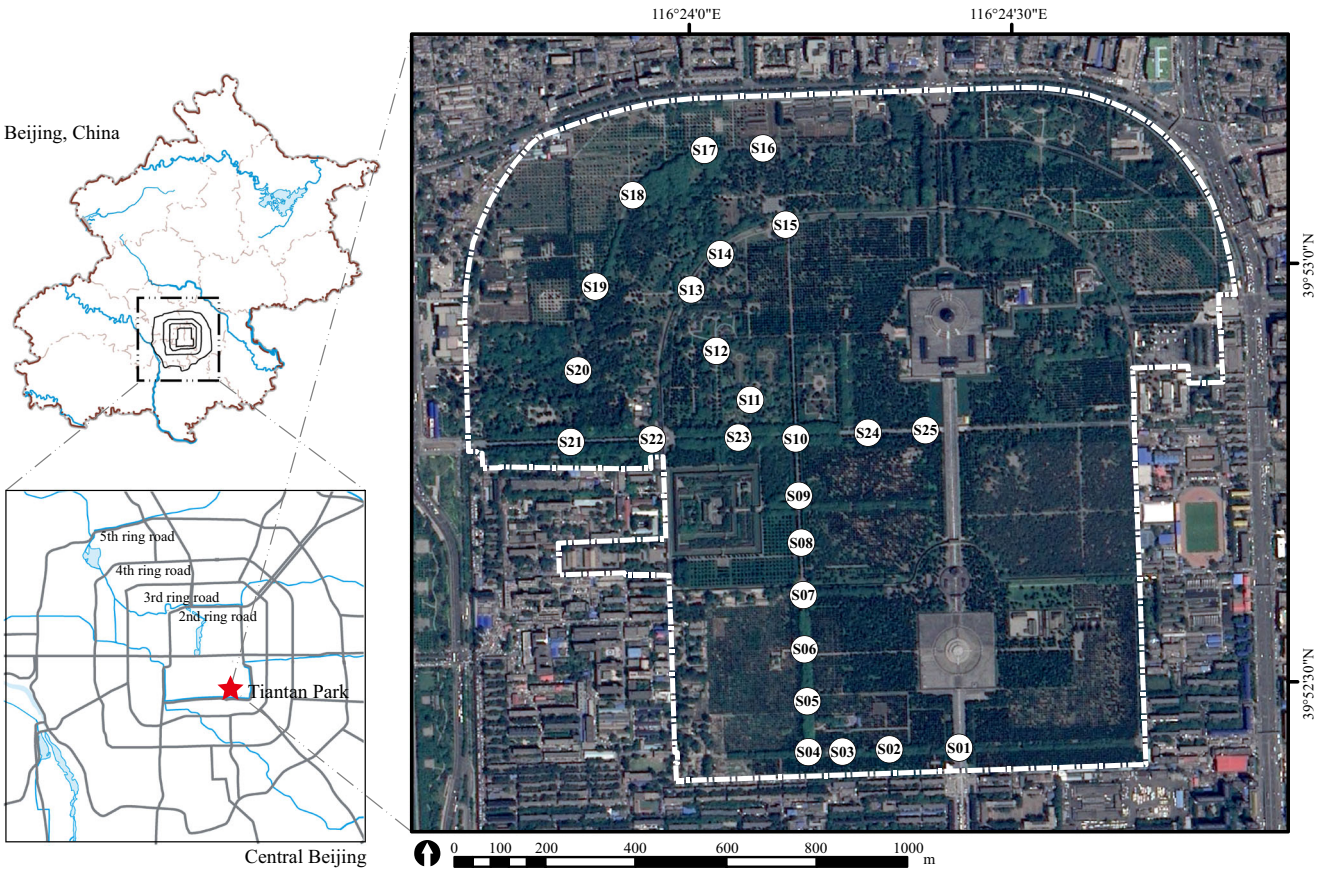

Fig. 1 Location of sampling points within Tiantan Park (The Temple of Heaven)

importing fisheye photos into RayMan v1.2 (Matzarakis et al. 2007), which had been widely used to analyze radiation condition and thermal comfort (He et al. 2015; Lin et al. 2012; Tan et al. 2013).

Land cover features is represented by percentage (PLAND) and average weighed mean shape index (AWMSI) of each land cover type within 25 m, 50 m and 100 m radius around each sampling point calculated by Fragstats 4.2.1 (McGarigal and Marks 1995) at class level. Previous research conducted by Yan et al. (2014a) has proved that land cover composition 20-50 m around the sampling points may best explain Ta in Beijing. Visual interpretation of imperious surfaces (IS), grassland (GL), deciduous tree (DT) and evergreen tree (ET) were conducted in Arc GIS 10.2 based on Worldview-3 and GF-2 image. There is no permanent bare land in the park. Shrubs were not identified because it is hardly possible to distinguish those shrubs under tree canopy through remote sensed data, and shrubs have limited impact on Ta and Rh under dense tree coverage (Prévosto et al. 2020). All 4 land cover types were used for the calculation of landscape metrics in summer, while 3 were used in winter, for the coverage of DT was divided into GL and IS. Definition and equation of landscape metrics are listed in Table 1.

Data analyses

Average Ta and Rh of 3 days were calculated, which further determined the ranges of Ta and Rh. One-way ANOVA was performed to compare Ta and Rh of each sampling points, before which we had already confirmed that they all complied with normal distribution and rejected Bartlett's test. R package Agricoae (Mendiburu 2017) was used to conduct Duncan multiple comparison at $\alpha = 0.05$.

For each sampling points, the average Ta and Rh of 3 days at noon and at night in summer and winter are calculated respectively. Pearson correlation between average Ta, Rh and all influencing factors were calculated by using R package Hmisc (Harrell 2018). Linear regression models were called for to estimate the trend between average Ta, Rh and correlated factors. Multiple linear regression models were built under stepwise algorithm to identify which influencing factor contribute the most to Ta and Rh within an urban park at different time, before which both dependent and independent variables were standardized so that the coefficients might effectively represent the order of importance. To avoid co-linearity among influencing factors, correlated factors or factors with similar meanings were removed from one same model.

All data analyses were conducted on R 3.5.3 (R Development Core Team 2015). Graphics were depicted in R and further edited in Adobe Illustrator when needed.

Table 2 Average and range of 3-day-averaged Ta and Rh of all sampling points in Tiantan Park

	Ta (°C)		Rh (%)	
	Average	Range	Average	Range
Summer noon	36.82	2.71	44.76	4.81
Summer night	32.71	1.29	57.71	5.16
Winter noon	6.08	1.47	16.91	1.27
Winter night	−2.45	2.21	35.37	5.03

Results

Spatial and temporal pattern of air temperature and relative humidity

The average and range of 3-day-averaged Ta and Rh among different sampling points are shown in Table 2, and the comparison of Ta and Rh are shown in Fig. 2. Significant differences are detected among Ta at noon in summer and at night in winter, as shown in Fig. 2, while no significant difference among Rh at all time. The range of Ta reaches as high as 2.71 °C at noon in summer, and the range of Rh reaches 5.16% at night in summer. Ta at noon in summer and Ta at night in winter are less evenly distributed. Ta of each sampling point is significantly different from at least 11 sampling points at noon in summer, and 15 sampling points at night in winter. Of all sampling points, the highest average Ta at noon in summer and winter were measured at S11, which features high SVF in both summer and winter and located near the center of Tiantan Park. It is also at S11 that a relatively lower Ta were detected at night in summer and winter. While no other sampling points show similar diurnal and nocturnal variation of Ta or Rh.

Table 1 Landscape metrics and calculation equations

Metric	Definition	Unit	Equation
PLAND	The percentage of each land cover type.	%	$PLAND = \frac{\sum_{j=1}^{n} a_{ij}}{A}$
AWMSI	The sum of the perimeter of each patch divided by the square root of patch area for each land cover type. AWMSI equals 1 when all patches are circular and increases when patches gain complexity in shape.	–	$AWMSI = \sum_{j=1}^{n}\left[\left(\frac{p_{ij}}{2\sqrt{\pi * a_{ij}}}\right)\left(\frac{a_{ij}}{\sum_{j=1}^{n} a_{ij}}\right)\right]$

a_{ij} refers to patch area of patch ij (m^2), p_{ij} refers to perimeter of patch ij (m), A refers to the total buffer area (m^2)

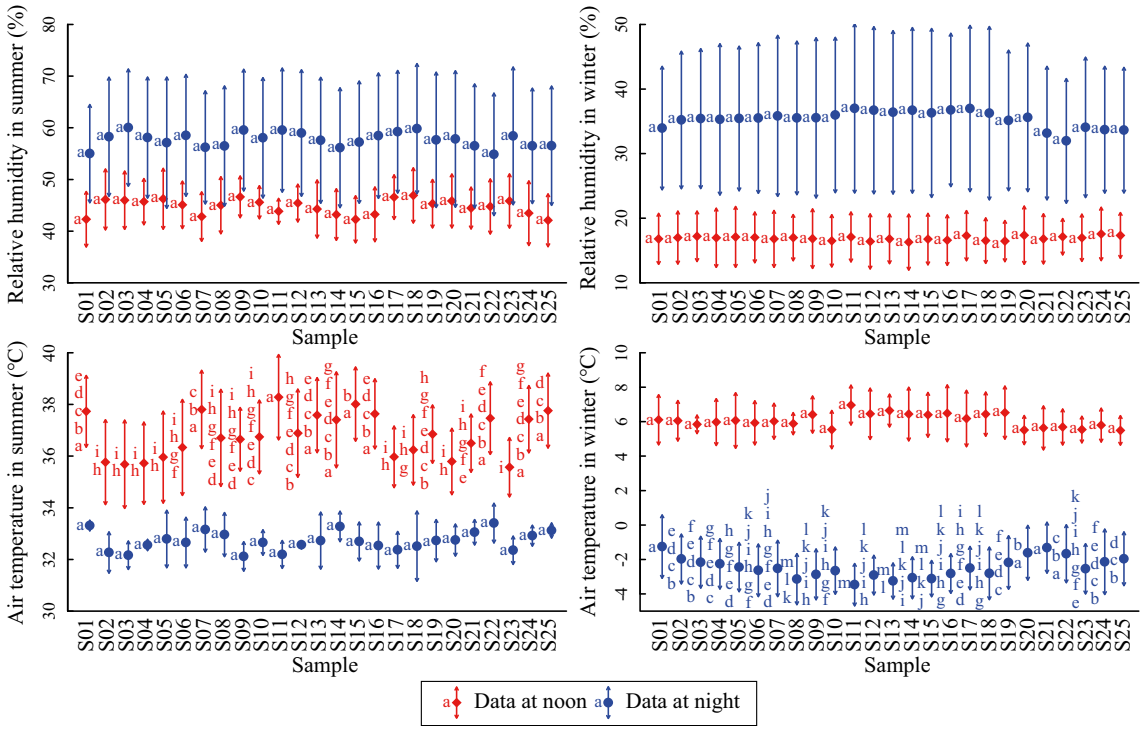

Fig. 2 Comparison of air temperature and relative humidity within Tiantan Park (Average with Standard deviation. Groups with identical letters are not significantly different at α = 0.05)

Spatial location of sampling points represented by their distance to park boundary and distance to park center has an impact on Ta. Table 3 shows significant Ta gradients at noon in summer and at night in winter within Tiantan Park. For every 100 m away from the park boundary, Ta at noon in summer shall rise 0.3 °C, as shown in Fig. 3a. While at night in winter, Ta shall drop 0.2 °C for every 100 m away from the park boundary, as shown in Fig. 3b.

Influence of radiation condition on air temperature and relative humidity

As Table 4 shows, radiation conditions above each sampling points are significantly correlated with daytime and nighttime Ta and Rh in summer and winter. Considering that sunshine duration and SVF are correlated parameters in both summer and winter ($\rho_{summer} = 0.901$ ($p < 0.01$), $\rho_{winter} = 0.838$ ($p < 0.01$)), and SVF is the parameter that is more closely related to design, it is selected for building linear models.

Ta at noon in both summer and winter and Ta at night in summer have a positive linear relationship with SVF, with the largest gradient at noon in summer, as shown in Fig. 4a-c. While Rh at noon in both summer and winter and Rh at night in summer have a negative linear relationship with SVF, with the largest gradient also at noon in summer, as shown in Fig. 4d-f. Ta and Rh at noon in summer are well explained by SVF, with R^2 as high as 0.861 and 0.606.

Influence of land cover features on air temperature and relative humidity

Thermal effects of different land cover types are different. As shown in Tables 5 and 6, among 3 different buffer scales, land cover features within 25 m may best explain Ta and Rh linearly, for their correlation coefficients are generally larger.

Table 3 Correlation coefficients between air temperature, relative humidity and spatial location of sampling points

	Summer				Winter			
	Rh at noon	Ta at noon	Rh at night	Ta at night	Rh at noon	Ta at noon	Rh at night	Ta at night
DTB	−0.35	**0.44***	−0.10	0.17	−0.01	0.09	0.18	**−0.45***
DTC	0.28	**−0.44***	0.08	−0.06	−0.10	0.09	0.07	0.39

*$p < 0.05$(two-tail); **$p < 0.01$(two-tail). *Rh* relative humidity, *Ta* air temperature, *DTB* distance to park boundary, *DTC* distance to park geometric center. Same below

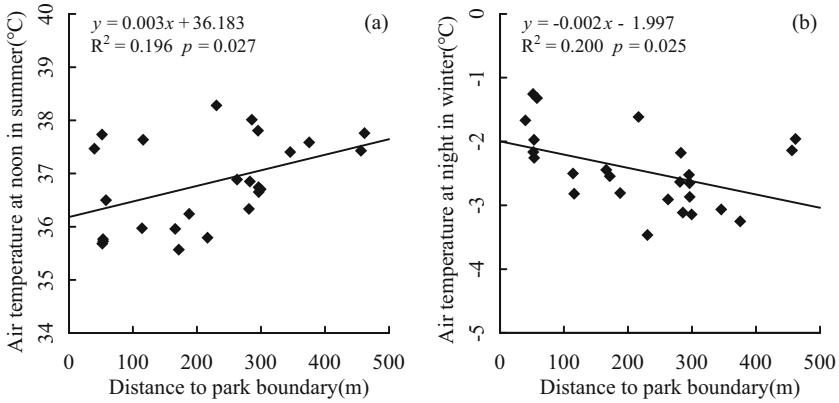

Fig. 3 Linear model with Ta as dependent variables and spatial location as independent variables

Higher percentage of IS and GL may both induce higher Ta at noon in summer. For 10% higher IS or GL coverage, Ta at noon in summer shall rise 0.03 °C (Fig. 5a-b). While at night in winter, IS and GL have opposite effects, with higher percentage of IS inducing higher Ta, and higher percentage of GL inducing lower Ta. At noon in summer, DT is the only element that may significantly reduce Ta and increase Rh. For 10% higher DT coverage, Ta at noon in summer shall drop 0.02 °C (Fig. 5c). ET, except for increasing Rh at noon in winter, barely have effects on micro scale climate within park area.

As shown in Table 6, more complexed IS may give rise to Ta at noon in summer and winter, while decrease Ta at night in winter. However, patch shape of all types of vegetation coverage is found have no impacts on microclimate within Tiantan park.

Dominant factor on air temperature and relative humidity

Table 7 demonstrates the multiple regression models between standardized Ta, Rh and influencing factors. Reliable models are built for daytime Ta in summer and winter, and nighttime Ta in winter.

Dominant influencing factor on Ta varies among time. Radiation condition represented by SVF has dominant impact on Ta during daytime. Ta at noon in summer is well explained by SVF and DTB ($R^2 = 0.90$), and SVF plays a more important role compared with DTB, with standardized coefficient 0.872. Ta at night in winter can be explained by SVF and percentage of GL and ET, also with SVF as the dominant influencing factor ($\beta = 0.723$). While during winter nighttime, land cover feature plays the most prominent role, with the standardized coefficient of percentage of pavement and building as high as 0.601.

Discussion

Air temperature and relative humidity variance within urban parks

Results of this research suggest that strong variance of Ta and Rh exists within Tiantan park. 1.29–2.71 °C Ta range and 1.27–5.16% Rh range at different time are in consistent with previous studies conducted in multiple cities (Cohen et al. 2012; Hwang et al. 2015; Bilgili et al. 2013). Significant Ta differences while insignificant Rh differences are detected within Tiantan Park (Fig. 2).

The different thermal properties of vegetation and imperious surfaces are the cause of microclimate difference in urban parks (Taha 1997). During daytime, imperious surfaces take in solar radiation and releases long-wave radiation which directly warm the air up, while vegetation may reduce the solar radiation that reaches the ground and consume energy through evapotranspiration (Grimmond and Oke 1991; Oke 1992).

Table 4 Correlation coefficients between air temperature, relative humidity and spatial location of sampling points

	Summer				Winter			
	Rh at noon	Ta at noon	Rh at night	Ta at night	Rh at noon	Ta at noon	Rh at night	Ta at night
SVF	**−0.78****	**0.93****	**−0.47***	**0.49***	**−0.43***	**0.51***	0.34	−0.28
SD	**−0.83****	**0.87****	**−0.51****	**0.50***	**−0.46***	**0.57****	**0.49***	**−0.40***

*$p < 0.05$(two-tail); **$p < 0.01$(two-tail). *SVF* sky view factor, *SD* sunshine duration

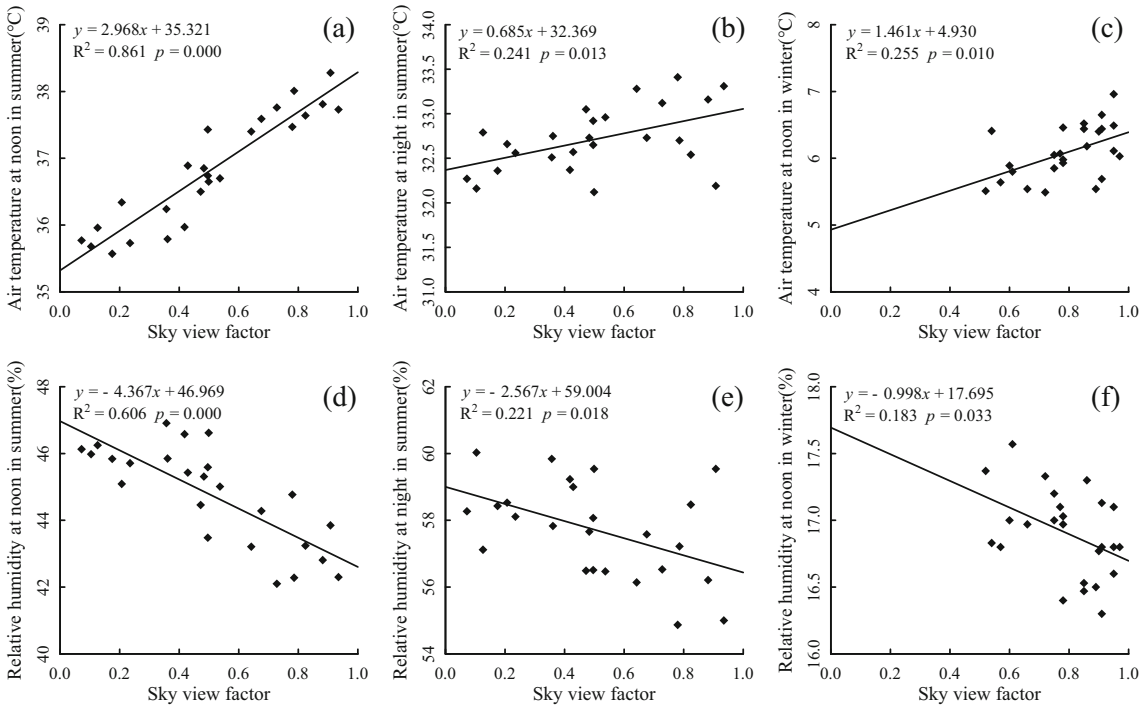

Fig. 4 Linear models with Ta and Rh as dependent variables and radiation condition as independent variables

More diversified Ta was observed during summer noon than night (Fig. 2). This complies with what Yan and Dong (2015) have also observed in Beijing that significant difference exists during summer daytime but not nighttime among woodland, grassland, paved area and water area. Vegetation was observed to have a mild warming effect at night for tree canopy may hinder long-wave radiation loss and affect ventilation (Jonsson 2004; Potchter et al. 2006; Chang and Li 2014), while Ta drops more rapidly above impervious surfaces and grassland, and thus resulting in a smaller Ta difference at night.

Based on the knowledge that vegetation may cool and humidify the environment while man-made surfaces have converse effects, one may draw the conclusion that the closer to

Table 5 Correlation coefficients among PLAND of different land cover types, air temperature and relative humidity

		Summer				Winter			
		Rh at noon	Ta at noon	Rh at night	Ta at night	Rh at noon	Ta at noon	Rh at night	Ta at night
IS	25 m	**−0.67** **	**0.65** **	**−0.68** **	**0.66** **	−0.03	−0.33	**−0.62** **	**0.51** **
	50 m	**−0.59** **	**0.68** **	**−0.66** **	**0.64** **	−0.04	−0.18	**−0.60** **	0.35
	100 m	**−0.49** *	**0.40** *	**−0.54** **	**0.49** *	0.06	−0.24	**−0.64** **	**0.51** **
GL	25 m	−0.25	**0.48** *	0.16	−0.16	**−0.46** *	**0.52** **	**0.75** **	**−0.62** **
	50 m	−0.24	**0.47** *	0.28	−0.22	**−0.42** *	**0.43** *	**0.65** **	**−0.49** *
	100 m	−0.13	0.36	0.27	−0.16	−0.36	**0.41** *	**0.61** **	**−0.53** **
DT	25 m	**0.62** **	**−0.65** **	0.39	−0.32	–	–	–	–
	50 m	**0.53** **	**−0.52** **	0.22	−0.15	–	–	–	–
	100 m	**0.44** *	**−0.40** *	0.22	−0.15	–	–	–	–
ET	25 m	−0.01	−0.10	−0.01	−0.06	**0.58** **	−0.29	−0.26	0.23
	50 m	0.03	−0.26	0.00	−0.09	**0.45** *	−0.30	−0.21	0.23
	100 m	0.01	−0.15	−0.07	−0.03	0.34	−0.28	−0.22	0.22

*$p < 0.05$(two-tail); **$p < 0.01$(two-tail). *Rh* relative humidity, *Ta* air temperature. *IS* imperious surfaces, *GL* grassland, *DT* deciduous tree, *ET* evergreen tree. Same below

Table 6 Correlation coefficients among AWMSI of different land cover types, air temperature and relative humidity

		Summer				Winter			
		Rh at noon	Ta at noon	Rh at night	Ta at night	Rh at noon	Ta at noon	Rh at night	Ta at night
IS	25 m	−0.32	**0.55** **	0.04	−0.03	**−0.51** **	**0.67** **	**0.54** **	**−0.74** **
	50 m	−0.33	**0.48** *	0.06	−0.09	**−0.48** *	0.31	0.36	**−0.61** **
	100 m	−0.25	**0.49** *	0.00	−0.06	**−0.45** *	0.35	**0.43** *	**−0.61** **
GL	25 m	0.19	−0.09	0.25	−0.20	−0.14	0.39	0.19	−0.32
	50 m	0.28	−0.19	0.34	−0.35	−0.24	0.28	0.24	−0.37
	100 m	0.21	−0.08	0.14	−0.11	−0.11	0.15	0.25	−0.37
DT	25 m	0.36	−0.27	0.31	−0.16	–	–	–	–
	50 m	0.29	−0.22	0.14	0.01	–	–	–	–
	100 m	0.14	−0.08	0.16	−0.01	–	–	–	–
ET	25 m	0.19	−0.23	−0.12	0.08	0.25	−0.28	−0.19	0.11
	50 m	0.08	−0.13	−0.28	0.28	0.15	−0.21	−0.08	0.15
	100 m	0.16	−0.24	−0.09	0.13	0.36	−0.30	0.01	0.08

*$p < 0.05$(two-tail); **$p < 0.01$(two-tail)

the park center, the lower Ta and the higher Rh will it be. Field measurement conducted by Barradas (1991) also depicted such gradients within urban parks. This is also in consistent with the widely-proved fact that urban parks are cold islands in cities, featuring lower Ta compared with its vicinity area (Bowler et al. 2010; Saaroni et al. 2018). However, Ta gradients at noon in summer in Tiantan Park does not comply with such conclusion, and Ta get higher as it gets closer to park center (Fig. 3a, Table 7 $\beta = 0.215$). One possible explanation is that park's landscape elements composition largely influenced the Ta gradients. The Ta map generated by Kriging method by Bilgili et al. (2013) also showed strong relevance to land composition. In this specific case of Tiantan Park, it may be attributed to the large area of impervious surfaces located at the park center, which counteracts the cooling effects of vegetation.

Vegetation's contribution on microclimate and implications for planting design

In an urban park as Tiantan Park that does not contain any water body, microclimate effects are mostly provided by vegetation through shading and evapotranspiration (Oke 1992; Taha et al. 1991). In this research, tree's shading effect is examined by radiation condition including SVF and SD, and is found to have the greatest contribution on reducing Ta during daytime (Table 7). Trees may reduce radiation absorbed by ground and therefore reduce long-wave radiation emission that may heat up the air (Dimoudi and Nikolopoulou 2003). Empirical researches widely prove that tree's shading have stable cooling effects in hot seasons in temperate, subtropical and tropical region (Ali and Patnaik 2019; Cohen et al. 2012; Hwang et al. 2015; Lin et al. 2013). Simulation

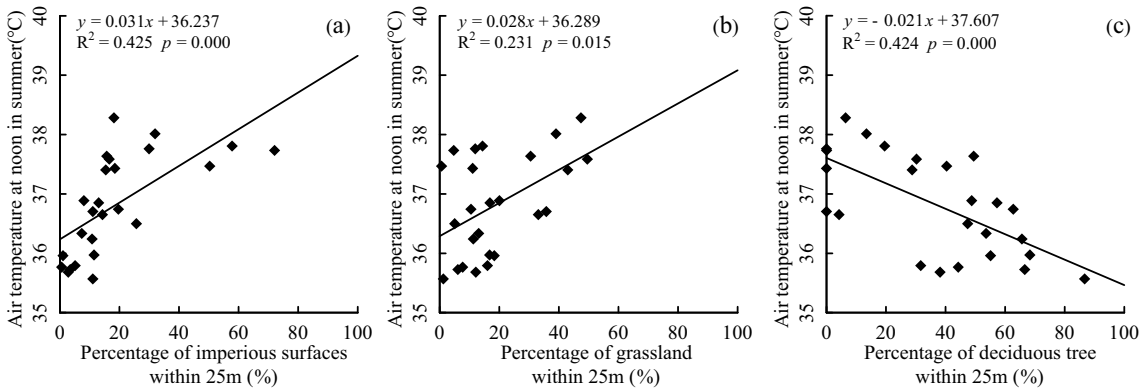

Fig. 5 Linear model with Ta as dependent variables and PLAND as independent variables

Table 7 Multiple regression results with air temperature as dependent variables

		Ta at noon in summer		Ta at noon in winter		Ta at night in winter	
		β	p	β	p	β	p
Spatial location	DTB	0.215	0.005**	–	–	−0.282	0.002**
Radiation condition	SVF	0.872	0.000**	0.723	0.002**	−0.528	0.079
Land cover	$PLANDIS_{25}$	–	–	–	–	0.601	0.001**
	$PLANDGL_{25}$	–	–	0.694	0.001**	–	–
	$PLANDET_{25}$	–	–	0.594	0.022*	–	–
	R^2	0.905		0.552		0.580	
	Adjusted R^2	0.899		0.488		0.521	
	p	<0.001**		0.001**		<0.001**	

*$p < 0.05$; **$p < 0.01$. β Standardized coefficient. $PLANDIS_{25}$ Percentage of imperious surfaces within 25 m buffer zone, $PLANDGL_{25}$ Percentage of grassland within 25 m buffer zone, $PLANDET_{25}$ Percentage of evergreen tree within 25 m buffer zone

and modelling studies also believe that tree's shading effect outweighs evapotranspiration on regulating microclimate (Manickathan et al. 2018), and shading is the most promising way to reduce heat load (Brown et al. 2015).

SVF is chosen for building linear models rather than SD, because SVF is more intuitive for landscape design. However, SVF is a geometry factor that cannot explicitly depict energy exchange, especially at mid to high latitude locations, where solar elevation angle may largely affect the radiation condition. While SD is a factor that is directly related to energy exchange. This may give explanation to our results that SD is generally better correlated with Ta and Rh than SVF (Table 4).

Trees cooling effect through shading is a double-edged sword, for it can enhance thermal environment in hot seasons while deteriorate it during cold times in a temperate climate (Cohen et al. 2012; Afshar et al. 2018). In winter, highly shaded areas endure much longer cold discomfort (He et al. 2015), while people generally desire more sunlight exposure (Xu et al. 2018). In order to enhance thermal comfort in winter, besides planting more deciduous trees to avoid winter shading, it is also crucial to select the best planting location. Several studies pointed out that $SVF_{90–270}$, which refers to SVF for the southern half of the upper hemisphere, is more closely related to direct solar radiation (Holst and Mayer 2011; Lee et al. 2013), and hence is more closely related to thermal comfort. It can be inferred that avoid planting evergreen trees directly to the south of travel route or squares may contribute to winter thermal comfort.

Different vegetation types also play different roles in regulating microclimate. Trees generally have the most pronounced effects, while turf or lawn has the least contribution to regulating Ta and Rh (Cheung and Jim 2019). It is reaffirmed that GL may increase Ta during daytime in summer and winter (Table 5), indicating thermally discomfortable in summer while the opposite in winter, as what Zhang et al. (2020) also observed. Results also indicate that deciduous trees may reduce Ta and increase Rh at noon in summer, while evergreen trees barely have any effects (Table 5). This may be attributed to the fact that the dominant evergreen tree species in Tiantan Park are cone-shaped conifers, such as *Juniperus chinensis* and *Platycladus orientalis*, which can barely cast any shade. Milošević et al. (2017) also found that cone-shaped trees have a weaker microclimate effect than sphere-shape trees through computer modelling. However, leaves of conifers are reported to have lower surface temperature and better cooling effects through evapotranspiration than deciduous trees (Leuzinger et al. 2010; Leuzinger and Körner 2007; Rana et al. 2020). This evidence may further prove that tree's shading outweighs evapotranspiration to provide better cooling effects. Additionally, we found that evergreen trees have a significant humidifying effect in winter, a phenomenon that is also found in Afshar et al. (2018) through numerical simulation. However, considering that people are less sensitive to RH in winter (Xu et al. 2018), the impact of such humidifying effect on thermal perception still awaits further investigation. Results of our work may provide empirical evidence for the microclimate effects of different vegetation types.

The configuration of different landscape elements including their proportion and shape is of great concern for designers. Enhancing vegetation coverage is a widely acknowledged method to enhance parks' thermal performance (Chang and Li 2014; Cheung and Jim 2019; Coseo and Larsen 2014), while it remains unclear how the shape of vegetation coverage affects its cooling and humidifying effects. We found that the shape of vegetation coverage has no impact on Ta or Rh (Table 6). However, studies using simulation method and remotely sensed data suggest that the shape of vegetation is linked with its thermal performance. Sodoudi et al. (2018) proves that belt-shaped tree coverage may provide best microclimate effects through simulation, and Yang et al. (2020) believes that

compact shape tree coverage may best regulate land surface temperature. How the shape of vegetation may affect Ta and Rh still requires further investment through empirical studies.

Conclusion

In this research, we took Tiantan Park in Beijing as a specimen and investigated Ta and Rh distribution within this park and related parameters through field measurements. Significant Ta variance and gradients were detected. Spatial location of, radiation condition above and land cover characteristics around each sampling points were found correlated with microclimate. Among all parameters, radiation condition is the dominant influencing factor on daytime Ta, while land cover characteristics is the dominant influencing factor on nighttime Ta in winter. Various microclimate effects are found among different vegetation types. Deciduous trees have a significant cooling and humidifying effect at noon in summer. While evergreen trees have little effects in summer, but a humidifying effect in winter. Grassland are found to increase daytime Ta in both summer and winter. Some of the above results are in consistent with previous simulation studies and mutual conclusions can be get. While the effects of the shape of different vegetation types remain unclear, and we found that a more compact IS may lead to lower daytime Ta. It can be inferred that besides enhancing vegetation coverage, less complex IS may lead to a more thermally comfort environment in summer. Choosing deciduous trees over evergreen ones and avoid planting evergreen trees directly to the south of where people tend to stay may potentially enhance thermal comfort in parks in winter.

Acknowledgements We acknowledge Dr. Xiaopeng Li and Dr. Hai Yan's assistance to review the first manuscript. We also want to thank the editors and anonymous reviewers for their delicate work.

Authors' contributions Conceptualization: Li Dong; Formal analysis: Yilun Li; Funding acquisition: Li Dong; Investigation: Yilun Li, Yue Zhang, Kun Li; Methodology: Yilun Li, Shuxin Fan; Project administration: Li Dong; Software: Yilun Li; Supervision: Li Dong; Writing-original draft: Yilun Li; Writing-review and and editing: Shuxin Fan, Kun Li, Li Dong.

Funding This study was funded by Beijing Municipal Science and Technology Commission (D171100007117001, D171100007217003).

Data availability Data will be made public under request.

Compliance with ethical standards

Ethics approval and consent to participate All data were collected in public space and no ethical issues encountered.

Consent for publication Not applicable.

Competing interests The authors have no conflicts of interest to declare that are relevant to the content of this article.

References

Afshar NK, Karimian Z, Doostan R, Nokhandan MH (2018) Influence of planting designs on winter thermal comfort in an Urban Park. J Environ Eng Landsc Manag 26:232–240. https://doi.org/10.3846/jeelm.2018.5374

Ali SB, Patnaik S (2019) Assessment of the impact of urban tree canopy on microclimate in Bhopal: a devised low-cost traverse methodology. Urban Clim 27:430–445. https://doi.org/10.1016/j.uclim.2019.01.004

Allen MR, Dube OP, Solecki W et al (2018) Framing and context. In: Masson-Delmotte V, Zhai P, Pörtner HO et al (eds) Global warming of 1.5°C. IPCC Special Report. https://www.ipcc.ch/sr15/chapter/chapter-1. Accessed 26 Nov 2020

Barradas VL (1991) Air temperature and humidity and human comfort index of some city parks of Mexico City. Int J Biometeorol 35:24–28. https://doi.org/10.1007/BF01040959

Bartesaghi Koc C, Osmond P, Peters A (2018) Evaluating the cooling effects of green infrastructure: a systematic review of methods, indicators and data sources. Sol Energy 166:486–508. https://doi.org/10.1016/j.solener.2018.03.008

Bilgili BC, Şahin Ş, Yilmaz O, Gürbüz F, Arici YK (2013) Temperature distribution and the cooling effects on three urban parks in an kara, Turkey. Int J Glob Warm 5:296–310. https://doi.org/10.1504/ijgw.2013.055364

Bowler DE, Buyung-Ali L, Knight TM, Pullin AS (2010) Urban greening to cool towns and cities: a systematic review of the empirical evidence. Landsc Urban Plan 97:147–155. https://doi.org/10.1016/j.landurbplan.2010.05.006

Brown RD, Vanos J, Kenny N, Lenzholzer S (2015) Designing urban parks that ameliorate the effects of climate change. Landsc Urban Plan 138:118–131. https://doi.org/10.1016/j.landurbplan.2015.02.006

Chang C-R, Li M-H (2014) Effects of urban parks on the local urban thermal environment. Urban For Urban Green 13:672–681. https://doi.org/10.1016/j.ufug.2014.08.001

Chang C-R, Li M-H, Chang S-D (2007) A preliminary study on the local cool-island intensity of Taipei city parks. Landsc Urban Plan 80:386–395. https://doi.org/10.1016/j.landurbplan.2006.09.005

Cheung PK, Jim CY (2019) Differential cooling effects of landscape parameters in humid-subtropical urban parks. Landsc Urban Plan 192:103651. https://doi.org/10.1016/j.landurbplan.2019.103651

Cohen P, Potchter O, Matzarakis A (2012) Daily and seasonal climatic conditions of green urban open spaces in the Mediterranean climate and their impact on human comfort. Build Environ 51:285–295. https://doi.org/10.1016/j.buildenv.2011.11.020

Coseo P, Larsen L (2014) How factors of land use/land cover, building configuration, and adjacent heat sources and sinks explain urban Heat Islands in Chicago. Landsc Urban Plan 125:117–129. https://doi.org/10.1016/j.landurbplan.2014.02.019

Costello A, Abbas M, Allen A, Ball S, Bell S, Bellamy R, Friel S, Groce N, Johnson A, Kett M, Lee M, Levy C, Maslin M, McCoy D, McGuire B, Montgomery H, Napier D, Pagel C, Patel J, de Oliveira JAP, Redclift N, Rees H, Rogger D, Scott J, Stephenson J, Twigg J, Wolff J, Patterson C (2009) Managing the health effects of climate change. Lancet 373:1693–1733. https://doi.org/10.1016/s0140-6736(09)60935-1

Dimoudi A, Nikolopoulou M (2003) Vegetation in the urban environment: microclimatic analysis and benefits. Energy Build 35:69–76. https://doi.org/10.1016/s0378-7788(02)00081-6

Gago EJ, Roldan J, Pacheco-Torres R, Ordóñez J (2013) The city and urban heat islands: a review of strategies to mitigate adverse effects. Renew Sust Energ Rev 25:749–758. https://doi.org/10.1016/j.rser.2013.05.057

Grimmond CSB, Oke TR (1991) An evapotranspiration-interception model for urban areas. Water Resour Res 27:1739–1755. https://doi.org/10.1029/91wr00557

Hami A, Abdi B, Zarehaghi D, Maulan SB (2019) Assessing the thermal comfort effects of green spaces: a systematic review of methods, parameters, and plants' attributes. Sustain Cities Soc 49:101634. https://doi.org/10.1016/j.scs.2019.101634

Harrell F (2018) Hmisc: Harrell Miscellaneous. R package version 4.1–1. https://CRAN.R-project.org/package=Hmisc. Accessed 26 Nov 2020

Hathway EA, Sharples S (2012) The interaction of rivers and urban form in mitigating the urban Heat Island effect: a UK case study. Build Environ 58:14–22. https://doi.org/10.1016/j.buildenv.2012.06.013

He X, Miao S, Shen S, Li J, Zhang B, Zhang Z, Chen X (2015) Influence of sky view factor on outdoor thermal environment and physiological equivalent temperature. Int J Biometeorol 59:285–297. https://doi.org/10.1007/s00484-014-0841-5

Holst J, Mayer H (2011) Impacts of street design parameters on human-biometeorological variables. Meteorol Z 20:541–552. https://doi.org/10.1127/0941-2948/2011/0254

Huang L, Li J, Zhao D, Zhu J (2008) A fieldwork study on the diurnal changes of urban microclimate in four types of ground cover and urban heat island of Nanjing, China. Build Environ 43:7–17. https://doi.org/10.1016/j.buildenv.2006.11.025

Hwang YH, Lum QJG, Chan YKD (2015) Micro-scale thermal performance of tropical urban parks in Singapore. Build Environ 94:467–476. https://doi.org/10.1016/j.buildenv.2015.10.003

International Standard Organization (1998) ISO 7726 thermal environments: instruments and methods for measuring physical quantities. ISO, Geneva

Jamei E, Rajagopalan P, Seyedmahmoudian M, Jamei Y (2016) Review on the impact of urban geometry and pedestrian level greening on outdoor thermal comfort. Renew Sust Energ Rev 54:1002–1017. https://doi.org/10.1016/j.rser.2015.10.104

Jansson C, Jansson PE, Gustafsson D (2007) Near surface climate in an urban vegetated park and its surroundings. Theor Appl Climatol 89:185–193. https://doi.org/10.1007/s00704-006-0259-z

Johansson E (2006) Influence of urban geometry on outdoor thermal comfort in a hot dry climate: a study in fez, Morocco. Build Environ 41:1326–1338. https://doi.org/10.1016/j.buildenv.2005.05.022

Jonsson P (2004) Vegetation as an urban climate control in the subtropical city of Gaborone, Botswana. Int J Climatol 24:1307–1322. https://doi.org/10.1002/joc.1064

Kong F, Yan W, Zheng G, Yin H, Cavan G, Zhan W, Zhang N, Cheng L (2016) Retrieval of three-dimensional tree canopy and shade using terrestrial laser scanning (TLS) data to analyze the cooling effect of vegetation. Agric For Meteorol 217:22–34. https://doi.org/10.1016/j.agrformet.2015.11.005

Lee H, Holst J, Mayer H (2013) Modification of human-biometeorologically significant radiant flux densities by shading as local method to mitigate heat stress in summer within urban street canyons. Adv Meteorol 2013:1–13. https://doi.org/10.1155/2013/312572

Leuzinger S, Körner C (2007) Tree species diversity affects canopy leaf temperatures in a mature temperate forest. Agric For Meteorol 146:29–37. https://doi.org/10.1016/j.agrformet.2007.05.007

Leuzinger S, Vogt R, Körner C (2010) Tree surface temperature in an urban environment. Agric For Meteorol 150:56–62. https://doi.org/10.1016/j.agrformet.2009.08.006

Lin T-P, Tsai K-T, Hwang R-L, Matzarakis A (2012) Quantification of the effect of thermal indices and sky view factor on park attendance. Landsc Urban Plan 107:137–146. https://doi.org/10.1016/j.landurbplan.2012.05.011

Lin T-P, Tsai K-T, Liao C-C, Huang Y-C (2013) Effects of thermal comfort and adaptation on park attendance regarding different shading levels and activity types. Build Environ 59:599–611. https://doi.org/10.1016/j.buildenv.2012.10.005

Liu W, Ji C, Zhong J, Jiang X, Zheng Z (2007) Temporal characteristics of the Beijing urban heat island. Theor Appl Climatol 87:213–221. https://doi.org/10.1007/s00704-005-0192-6

Management Office of the Temple of Heaven (2002) History of the Temple of heaven (in Chinese). China Forestry Press, Beijing

Manickathan L, Defraeye T, Allegrini J, Derome D, Carmeliet J (2018) Parametric study of the influence of environmental factors and tree properties on the transpirative cooling effect of trees. Agric For Meteorol 248:259–274. https://doi.org/10.1016/j.agrformet.2017.10.014

Masoudi M, Tan PY (2019) Multi-year comparison of the effects of spatial pattern of urban green spaces on urban land surface temperature. Landsc Urban Plan 184:44–58. https://doi.org/10.1016/j.landurbplan.2018.10.023

Matzarakis A, Rutz F, Mayer H (2007) Modelling radiation fluxes in simple and complex environments–application of the RayMan model. Int J Biometeorol 51:323–334. https://doi.org/10.1007/s00484-006-0061-8

McGarigal K, Marks BJ (1995) FRAGSTATS: Spatial pattern analysis program for quantifying landscape structure. Gen Tech Rep, PNW-GTR-351. https://doi.org/10.2737/PNW-GTR-351

Mendiburu F (2017) Agricolae: Statistical Procedures for Agricultural Research. R package version 1.2-8. https://CRAN.R-project.org/package=agricolae. Accessed 26 Nov 2020

Milošević DD, Bajšanski IV, Savić SM (2017) Influence of changing trees locations on thermal comfort on street parking lot and footways. Urban For Urban Green 23:113–124. https://doi.org/10.1016/j.ufug.2017.03.011

Morakinyo TE, Kong L, Lau KK-L, Yuan C, Ng E (2017) A study on the impact of shadow-cast and tree species on in-canyon and neighborhood's thermal comfort. Build Environ 115:1–17. https://doi.org/10.1016/j.buildenv.2017.01.005

National Bureau of Statistics of China (Beijing) (2018) Beijing statistical yearbook 2017. China Statistics Press, Beijing

Oke TR (1992) Boundary layer climate, 2nd edn. Methuen, London

Oke TR, Crowther JM, McNaughton KG, Monteith JL, Gardiner B (1989) The micrometeorology of the urban forest. Philos Trans R Soc B-Biol Sci 324:335–349. https://doi.org/10.1098/rstb.1989.0051

Patz JA, Campbell-Lendrum D, Holloway T, Foley JA (2005) Impact of regional climate change on human health. Nature 438:310–317. https://doi.org/10.1038/nature04188

Peng J, Xie P, Liu Y, Ma J (2016) Urban thermal environment dynamics and associated landscape pattern factors: a case study in the Beijing metropolitan region. Remote Sens Environ 173:145–155. https://doi.org/10.1016/j.rse.2015.11.027

Potchter O, Cohen P, Bitan A (2006) Climatic behavior of various urban parks during hot and humid summer in the mediterranean city of Tel Aviv, Israel. Int J Climatol 26:1695–1711. https://doi.org/10.1002/joc.1330

Prévosto B, Helluy M, Gavinet J, Fernandez C, Balandier P (2020) Microclimate in Mediterranean pine forests: what is the influence of the shrub layer? Agric For Meteorol 282-283:107856. https://doi.org/10.1016/j.agrformet.2019.107856

R Development Core Team (2015) R: A language and environment for statistical computing. http://www.r-project.org/

Rana G, De Lorenzi F, Mazza G, Martinelli N, Muschitiello C, Ferrara RM (2020) Tree transpiration in a multi-species Mediterranean garden. Agric For Meteorol 280:107767. https://doi.org/10.1016/j.agrformet.2019.107767

Saaroni H, Amorim JH, Hiemstra JA, Pearlmutter D (2018) Urban green infrastructure as a tool for urban heat mitigation: survey of research methodologies and findings across different climatic regions. Urban Clim 24:94–110. https://doi.org/10.1016/j.uclim.2018.02.001

Saaroni H, Ziv B (2003) The impact of a small lake on heat stress in a Mediterranean urban park: the case of Tel Aviv, Israel. Int J Biometeorol 47:156–165. https://doi.org/10.1007/s00484-003-0161-7

Sodoudi S, Zhang H, Chi X, Müller F, Li H (2018) The influence of spatial configuration of green areas on microclimate and thermal comfort. Urban For Urban Green 34:85–96. https://doi.org/10.1016/j.ufug.2018.06.002

Sun R, Chen L (2017) Effects of green space dynamics on urban heat islands: mitigation and diversification. Ecosyst Serv 23:38–46. https://doi.org/10.1016/j.ecoser.2016.11.011

Sun S, Xu X, Lao Z, Liu W, Li Z, Higueras García E, He L, Zhu J (2017) Evaluating the impact of urban green space and landscape design parameters on thermal comfort in hot summer by numerical simulation. Build Environ 123:277–288. https://doi.org/10.1016/j.buildenv.2017.07.010

Taha H (1997) Urban climates and heat islands: albedo, evapotranspiration, and anthropogenic heat. Energy Build 25:99–103. https://doi.org/10.1016/s0378-7788(96)00999-1

Taha H, Akbari H, Rosenfeld A (1991) Heat island and oasis effects of vegetative canopies: micro-meteorological field-measurements. Theor Appl Climatol 44:123–138. https://doi.org/10.1007/bf00867999

Taleghani M, Tenpierik M, van den Dobbelsteen A, Sailor DJ (2014) Heat in courtyards: a validated and calibrated parametric study of heat mitigation strategies for urban courtyards in the Netherlands. Sol Energy 103:108–124. https://doi.org/10.1016/j.solener.2014.01.033

Tan CL, Wong NH, Jusuf SK (2013) Outdoor mean radiant temperature estimation in the tropical urban environment. Build Environ 64:118–129. https://doi.org/10.1016/j.buildenv.2013.03.012

Toparlar Y, Blocken B, Maiheu B, van Heijst GJF (2017) A review on the CFD analysis of urban microclimate. Renew Sust Energ Rev 80:1613–1640. https://doi.org/10.1016/j.rser.2017.05.248

Toparlar Y, Blocken B, Maiheu B, van Heijst GJF (2018) The effect of an urban park on the microclimate in its vicinity: a case study for Antwerp, Belgium. Int J Climatol 38:e303–e322. https://doi.org/10.1002/joc.5371

United Nations, Department of Economic and Social Affairs, Population Division (2019) World urbanization prospects: the 2018 revision. United Nations, New York

Xu X, Cai H, Qiao Z, Wang L, Jin C, Ge Y, Wang L, Xu F (2017) Impacts of park landscape structure on thermal environment using QuickBird and Landsat images. Chin Geogr Sci 27:818–826. https://doi.org/10.1007/s11769-017-0910-xs

Xu M, Hong B, Mi J, Yan S (2018) Outdoor thermal comfort in an urban park during winter in cold regions of China. Sustain Cities Soc 43:208–220. https://doi.org/10.1016/j.scs.2018.08.034

Yan H, Dong L (2015) The impacts of land cover types on urban outdoor thermal environment: the case of Beijing, China. J Environ Health Sci Eng 13:43. https://doi.org/10.1186/s40201-015-0195-x

Yan H, Fan S, Guo C, Hu J, Dong L (2014a) Quantifying the impact of land cover composition on intra-urban air temperature variations at a mid-latitude city. PLoS One 9:e102124. https://doi.org/10.1371/journal.pone.0102124

Yan H, Fan S, Guo C, Wu F, Zhang N, Dong L (2014b) Assessing the effects of landscape design parameters on intra-urban air temperature variability: the case of Beijing, China. Build Environ 76:44–53. https://doi.org/10.1016/j.buildenv.2014.03.007

Yan H, Wu F, Dong L (2018) Influence of a large urban park on the local urban thermal environment. Sci Total Environ 622-623:882–891. https://doi.org/10.1016/j.scitotenv.2017.11.327

Yang G, Yu Z, Jørgensen G, Vejre H (2020) How can urban blue-green space be planned for climate adaption in high-latitude cities? A seasonal perspective. Sustain Cities Soc 53:101932. https://doi.org/10.1016/j.scs.2019.101932

Zhang L, Wei D, Hou Y, Du J, Za L, Zhang G, Shi L (2020) Outdoor thermal comfort of Urban Park—a case study. Sustainability 12. https://doi.org/10.3390/su12051961